A monolithic compliant large-range gravity balancer

Radaelli, Giuseppe; Herder, Just

DOI
10.6567/IFToMM.14TH.WC.OS20.018

Publication date
2015

Document Version
Final published version

Published in
Proceedings of the 14th IFToMM World Congress

The 14th IFToMM World Congress, Taipei, Taiwan, October 25-30, 2015
DOI Number: 10.6567/IFToMM.14TH.WC.OS20.018

A Monolithic Compliant Large-Range Gravity Balancer

G. Radaelli*, J. L. Herder†
Dept. Precision and Microsystems Engineering
Delft University of Technology
Delft, The Netherlands

Abstract—*A new monolithic fully compliant gravity balancer is designed with help of a design approach based on shape optimization. The balancer consists of one single complex-shaped beam on which the weight is attached. The beam is modeled as a planar isogeometric Bernoulli beam. The goal function of the optimization consists of an energy based evaluation of the load path of the beam which is compared with a desired response. The best result of the shape optimization has been constructed out of polycarbonate sheet and has been tested on a compression test bench. The experimental results have good resemblance with the theoretical model.*

Keywords: compliant mechanisms, static balancing, constant force generator

I. Introduction

Compliant mechanisms, i.e. mechanisms that achieve their motion from the deflection of their members instead of from kinematic constraints [1], are more challenging to design due to their inherent coupling between kinetics and kinematics. Designers often find their way to lumped parameter models like e.g. pseudo-rigid-body models (PRBM) [2] [3] [4], in order to deal with these challenges, but giving up in terms of accuracy, freedom of shape, and moreover often basing their designs on equivalent rigid body mechanism designs.

Statically balanced compliant mechanisms (SBCM) [5] are a subset of compliant mechanisms where undesired forces are compensated by elastic forces generated by the deflection of the mechanism. In these and other types of mechanisms it is often desirable to follow a required force-displacement path with good accuracy in order to enhance the quality of balancing and thus its performance. Examples where following a force displacement path is relevant can be found in [6] [7] [8] [9].

Recently a design approach has been proposed by the authors [10][11] that enables the design of compliant mechanisms with prescribed load-paths with good accuracy and great flexibility of shape. The method is based on shape optimization of elastic structures undergoing large deflections modeled through the isogeometric analysis (IGA) framework [12]. This is an emerging framework allied to the finite element method (FEM), but with increased accuracy and efficiency especially due to the absence of a conversion step between CAD geometry and analysis geometry.

In the current work a design has been generated through the use of the proposed design approach based on shape optimization, and validated by the construction and measurements of a physical model. The purpose of this design is to balance a weight, or constant force, over a fairly large vertical displacement without restricting the horizontal motion of the weight. The model consists of a fully distributed and monolithic compliant mechanism, that consists of a single branch prismatic beam.

The paper also presents the measurements setup, where the challenge is applying and measuring a solely vertical force while not restraining the horizontal motion.

The paper is structured as follows. Next section (II) shows the design method, and formulation of the design problem. In section III the design resulting from the optimization is shown. Section IV illustrates the design of the measurement setup and section V shows the measurements results. Concluding the paper, sections VI and VII contain the discussion and conclusions.

II. Method

The current section describes the formulation of the design problem and discusses some inputs for the design approach, suggested in [11].

A. Problem formulation

A.1 Goal

The goal of the design procedure is to find a compliant mechanism of which a selected point L is displaced downwards resulting in a constant upward vertical force over a given range. Consequently, this constant force can be replaced by a weight obtaining a statically balanced system.

Considering a quasi-static and conservative mechanical system, a constant force mechanism is one that possesses a linearly increasing potential energy with respect to the displacement at the point of application of the force and in its direction. For this purpose we define the array of obtained potential energy as

$$\mathbf{U} = \left[\; U_1(\delta_1) \quad U_2(\delta_2) \quad ... \quad U_m(\delta_m) \; \right] \qquad (1)$$

*G.Radaelli@tudelft.nl
†J.L.Herder@tudelft.nl

where U_k are the values of the potential energy of the system in an equilibrium situation corresponding to the applied displacement δ_k at step k. In this case δ_k, $k = 1..m$ is a discrete set of linearly spaced vertical displacements of the selected point.

Since it is not the shape but the sizing of the resulting design that will be mostly responsible for the magnitude of the constant force to be balanced, i.e. the payload, the goal function will be made independent of the amplitude by normalization. This is done by scaling the array of obtained energy values $\mathbf{U}$ so to meet the requirement that the minimum value corresponds to zero and the maximum value corresponds to one. The scaled energy array is obtained by scaling every entry of $\mathbf{U}$ according to

$$\tilde{U}_k = \frac{U_k - U_{min}}{U_{max} - U_{min}} \quad k = 1..m \ . \tag{2}$$

The reference array to be compared with, also bounded between zero and one, is a linearly increasing sequence

$$\hat{U}_k = \frac{k-1}{m-1} \quad k = 1..m \ . \tag{3}$$

The goal function to be optimized is formulated as

$$f_0 = \frac{\left(\tilde{\mathbf{U}} - \hat{\mathbf{U}}\right)\left(\tilde{\mathbf{U}} - \hat{\mathbf{U}}\right)^T}{\hat{\mathbf{U}}\hat{\mathbf{U}}^{\mathbf{T}}} \tag{4}$$

This is equivalent to the normalized sum of squared errors.

There is an initial build up of the vertical force expected since the system starts from equilibrium. This build up is desired to be short and steep, to keep the constant force region as large as possible. In terms of energy this means that the slope goes from initially zero to a certain slope which from that point on is desired to be kept constant. These initial steps of build-up will influence the goal function negatively and are therefore omitted in above expressions. The amount of steps to be omitted is a choice up to the designer.

A.2 Model

The mechanical model that has been used is that of a single beam clamped between the two endpoints. The beam is modeled by an isogeometric, geometrically nonlinear Bernoulli beam [13], with a linear material constitutive law, of which the potential energy is evaluated at every imposed boundary condition.

In the isogeometric formulation a B-spline with relatively small amount n of control points $\mathbf{B}_i$, with $i = 1..n$, describes the geometry of the beam, see Fig. 1. Consequently the shape is refined in a B-spline with a larger amount r of control points $\mathbf{P}_i$, with $i = 1..r$, for the analysis, where the displacements of the control points represent the degrees of freedom of the system.

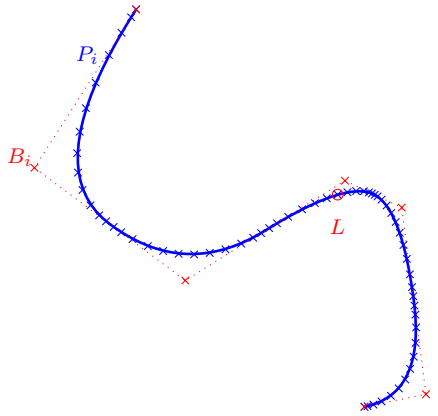

Fig. 1: B-spline with original control points $\mathbf{B}_i$, with $i = 1..n$, refined control points $\mathbf{P}_i$, with $i = 1..r$, and point of displacement application L.

The vertical displacement is applied at the central control point of the refined B-spline, point L. Strictly taken, this is not the same as applying a displacement on a point on the curve itself, since the B-spline is generally not interpolatory, i.e. the curve generally does not intersect the control points. However, the offset between control points and curve becomes smaller as the number or control points increases. In practice, applying a refinement up to more than 30 control points, makes the distance insignificant, here less then $0.1mm$ on a $300mm$ scale model, compared with e.g. fabrication and other errors.

In the presented analysis the shape is determined by $n = 7$ control points and is refined to $r = 50$ control points.

Considering that the application of the mechanism includes the effect of gravity on the payload, it is recommendable to include also the self-weight of the beam into the energy functional. This is done by introducing the mass matrix [13] that can be evaluated from

$$\mathbf{M}(i,j) = \int \rho A R_i R_j J d\xi \tag{5}$$

where i and j, the matrix indexes, correspond to every position of the control ponts, i.e. the degrees of freedom. Moreover ρ is the material density, $A(\xi)$ is the cross-sectional area, R_i is the basis function corresponding to the $i-th$ control point, J is the jacobian and ξ is the parameter of the curve. The gravitational potential energy term is calculated as the product of the gravitational acceleration g, here zero in horizontal direction, the mass matrix, and the current position of the control points.

$$U_g = g\mathbf{MP} \tag{6}$$

The total potential energy is now simply given by the sum of the elastic energy and the gravitational energy

$$U = U_g + U_e \tag{7}$$

B. Shape optimization

B.1 Optimization parameters

The set of control points $\mathbf{B}$ of the upper-level B-spline are the parameters of the optimization. For convenience in the applications of bounds for the optimization and interpretation of the results, the positions of the control points are re-parameterized according to

$$\mathbf{B} = \begin{bmatrix} B_{1_x} \\ B_{1_y} \\ B_{2_x} \\ B_{2_y} \\ B_{3_x} \\ B_{3_y} \\ B_{4_x} \\ B_{4_y} \\ \vdots \end{bmatrix} = \begin{bmatrix} q_1 \\ q_2 \\ q_1 + q_3 c\left(q_4\right) \\ q_2 + q_3 s\left(q_4\right) \\ q_1 + q_3 c\left(q_4\right) + q_5 c\left(q_4 + q_6\right) \\ q_2 + q_3 s\left(q_4\right) + q_5 s\left(q_4 + q_6\right) \\ q_1 + \ldots + q_7 c\left(q_4 + q_6 + q_8\right) \\ q_2 + \ldots + q_7 s\left(q_4 + q_6 + q_8\right) \\ \vdots \end{bmatrix} \tag{8}$$

where c and s are the shorthand notations for cos and sin, and $\mathbf{q}$ defined as

$$\mathbf{q} = \begin{bmatrix} B_{1_x} & B_{1_y} & l_1 & \theta_1 & l_2 & \theta_2 & l_3 & \theta_3 & \ldots \end{bmatrix}. \tag{9}$$

This transforms the parameters of optimization from an array of Cartesian coordinates to a sequence of lengths l_k and relative angles θ_k, i.e. it describes the control polygon of the spline as if it were a linkage chain, see Fig. 2. By this transformation it becomes easy to apply limits to the search space. For example, limiting the angles avoids sharp corners in the beam. Additionally giving a lower limit to the lengths also helps avoiding loops of the spline which in practice leads to unfeasible structures.

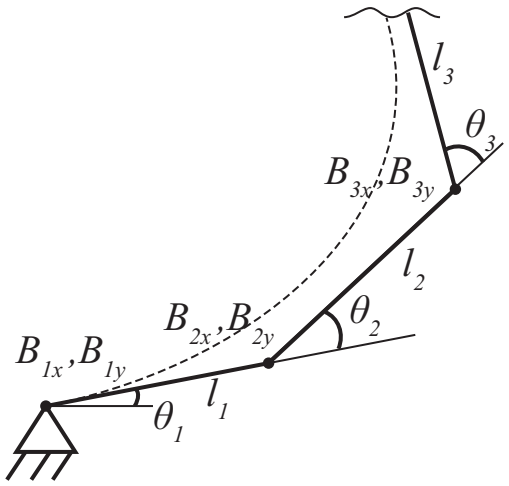

Fig. 2: Transformation of coordinates of the control points in a set of generalized coordinates, described by the lengths and angles of the links of a linkage chain, representing the control polygon.

parameter	value	units
E	25	$[GPa]$
ρ	2000	$[kg/m^3]$
width	0.15	$[m]$
thickness	0.002	$[m]$

TABLE I: Material and sizing parameters

In the current optimization a control polygon of 7 control points is used. The first two parameters of vector $\mathbf{q}$, i.e. the position of the begin of the beam, are fixed to zero. In this particular case these parameters only determine the global position of the mechanism in space and have no influence on its behavior. This results in 12 optimization parameters of which 6 are the lengths of the control polygon sides and 6 are their relative angles.

B.2 Sizing parameters

The optimization is performed on the shape parameters only, while sizing parameters are kept out of consideration by normalizing for an undetermined payload, as discussed. As soon as the shape is found it is possible to change the sizing variables, i.e. the cross-section dimensions and the Young's modulus, to match a desired payload. As long as the Euler-Bernoulli conditions, i.e. $length >> thickness$, are met, the sizing will not influence the balancing results.

The dimensions and properties used as starting point in current optimization run are given in table I, meant for a glass fiber reinforced plastic slender beam construction.

B.3 Algorithm

The selected optimization algorithm is the Sequential Quadratic Programming (SQP) from the Matlab® *Optimization Toolbox*, started at 50 different starting point randomly distributed around the search space using the *MultiStart* option in the *Global Optimization Toolbox*.

The sensitivities of the shape variables are calculated in an analytical fashion following the procedure described in [11].

The search space of the algorithm is bounded to avoid loops and sharp corners in the beam. This is accomplished by bounding the lengths of the sides of the control polygon between 0.05 $[m]$ and 0.15 $[m]$, and their relative angles between -2 $[rad]$ and 2 $[rad]$. Th total vertical applied displacement is 0.21 $[m]$.

III. Optimization Results

Out of the 50 runs from different random starting points the best result has been selected. For this run the converged solution $\mathbf{q}_{end}$ is shown in table II. The behavior of the optimized geometry is shown in Fig. 3, showing the undeformed geometry in red (thick line) and the deformed geometries corresponding to every displacement step in blue

Par. name	Unit	$\mathbf{q}_{end}$
B_{1_x}	$[mm]$	0.00
B_{1_y}	$[mm]$	0.00
l_1	$[mm]$	85.8
θ_1	$[rad]$	1.23
l_2	$[mm]$	10.8
θ_2	$[rad]$	0.06
l_3	$[mm]$	12.6
θ_3	$[rad]$	1.54
l_4	$[mm]$	05.1
θ_4	$[rad]$	0.73
l_5	$[mm]$	12.9
θ_5	$[rad]$	1.24
l_6	$[mm]$	11.9
θ_6	$[rad]$	0.01

TABLE II: Optimized design vector

(thin lines). The red crosses are the control points of the design vector and the red circle is the point of application of the vertical displacement. Figure 4 shows the optimized energy graph (blue circled) compared to the reference energy (red crossed). Since the difference between the obtained and reference energy is hardly visible, the error between both is plotted in Fig. 5. The final objective function, i.e. the normalized sum of squared errors, is $1.48e-4$. The resulting reaction force in vertical direction due to the applied displacement is plotted in Fig. 6. Finally an overview of the strains is provided in Fig. 7. Here for every load step the energy is drawn for the innermost material layer (green) and the outermost layer (blue). On the horizontal axis the parameter of the b-spline is en which ranges from 0 to 1 from the begin to the end of the curve.

IV. Experimental evaluation

In the current section the construction of the physical model is shortly presented and the measurements setup explained.

A. Prototype Construction

As a preliminary investigation before making a glass-fiber reinforced plastic version of the beam, as foreseen in the optimization material parameters, a polycarbonate version of the same beam is constructed. Polycarbonate is broadly available, cheap and has fairly good mechanical properties. Moreover the process is fairly simple and leads quickly to acceptable results. Two beams have been constructed with different plate thicknesses: 1 mm and 2 mm. A one-sided mould is cnc-milled out of high-density foam material, see Fig. 8. Then a polycarbonate plate is heated above its glass-transition temperature and then draped onto the mould. When the plastic reaches ambient temperature

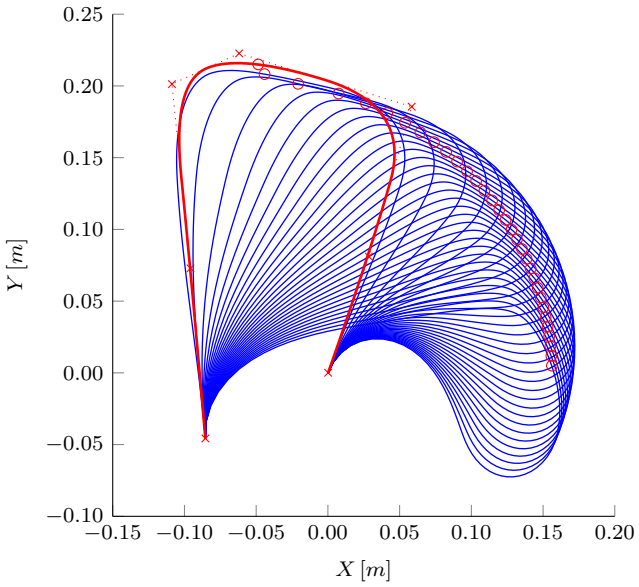

Fig. 3: Undeformed geometry of the optimized shape (red) and deformed geometries corresponding to every displacement step(blue). The red dot indicates the point of application of the vertical displacement.

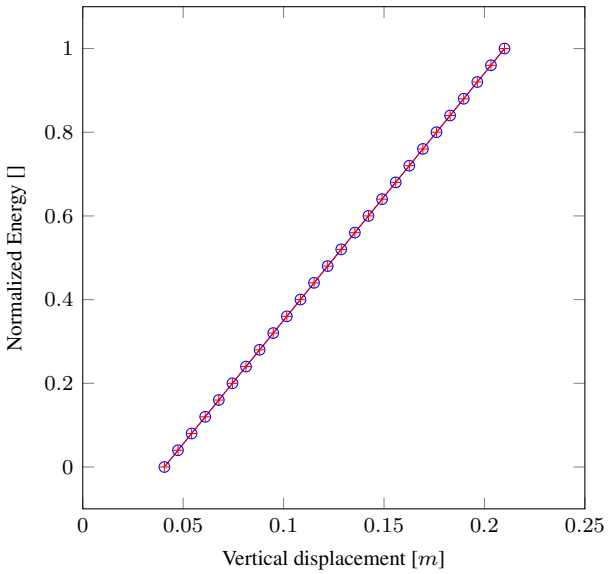

Fig. 4: Optimized energy graph (blue circled) and reference energy graph (red crossed).

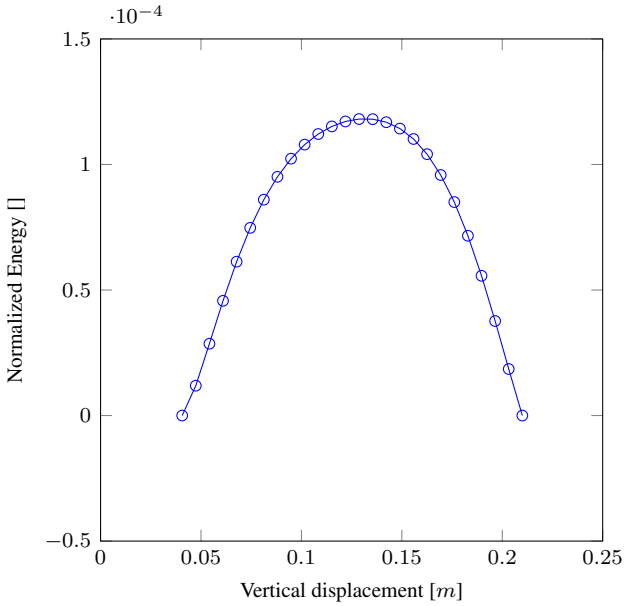

Fig. 5: Error between optimized energy graph and reference energy graph.

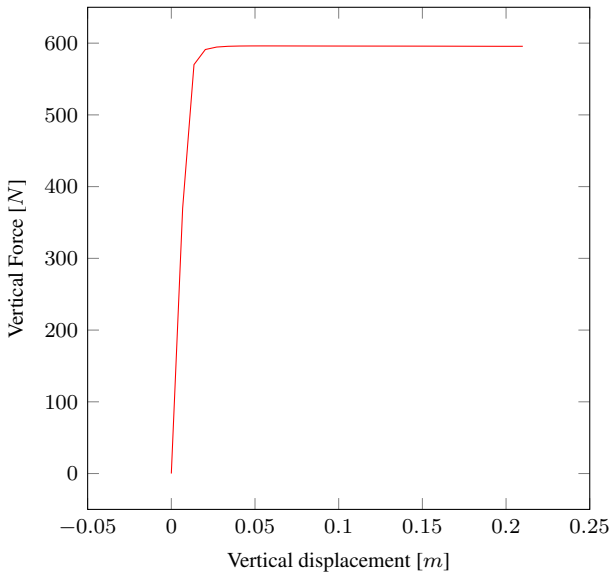

Fig. 6: Optimized vertical force vs displacement diagram.

again, the beam is ready to be clamped onto the supporting structure, see Fig. 9.

B. Measurements Setup

For the experimental evaluation the vertical reaction force is measured while a displacement is applied at the selected point. It is important that only a vertical displacement is applied, while the horizontal motion of that point is completely free. This is a challenge for conventional compression testing machines that travel along a straight line. To overcome this limitation, the base of the compliant mechanism was made to be mobile by placing it on a 2D planar stage. This stage consists of two sets of orthogonally placed rollers that effect the planar translations with negligible friction (planar rotation was not accommodated). As shown in Fig. 10 two long steel rollers are placed parallel in the direction of motion of the support of the beam. Other two rollers are placed in perpendicular direction on top of the first set of rollers. Again other two rollers are placed in the direction of motion right underneath the support base of the beam. The roller configuration is chosen such that only point contacts are made between rolling parts and that the reaction force is always within the support polygon of these point contacts. The only motion in the horizontal plane that is restricted is the rotation. However, no such rotational motion is expected in this design, and no such tendency is observed during the measurements.

The interface between the beam and the load cell has been designed such that the applied displacement is nicely distributed along a line corresponding to the selected point

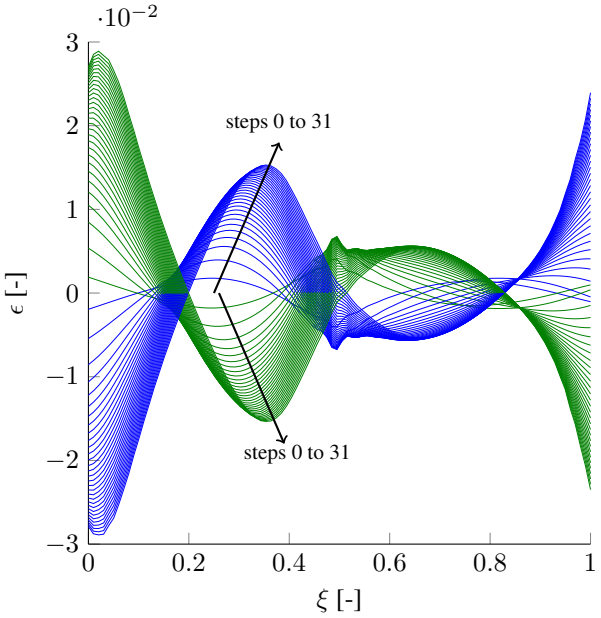

Fig. 7: Material strains for a $2mm$ thick plate. The lines represent the strain across the length of the beam, from curve parameter $\xi = 0$ to $\xi = 1$. The green lines represent the innermost material layer and the blue lines represents the outermost material layer. The lines are drawn for every load step.

Fig. 8: One sided mould out of high-density foam material.

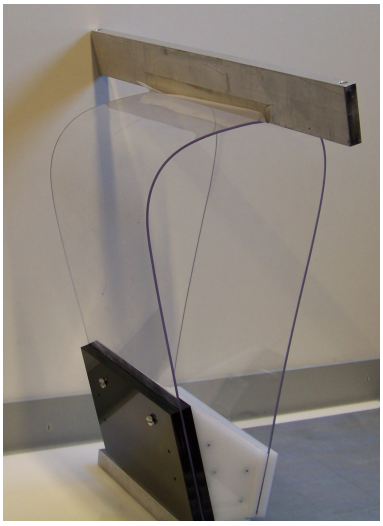

Fig. 9: Polycarbonate beam clamped onto support structure.

in the planar representation of the beam. This has been achieved by a knife-edge bearing, created by a rectangular prismatic aluminum bar that makes contact with the beam only at one lower corner, see Fig. 11. This contact is maintained during the whole range of motion. The position of the contact line on the beam is maintained by a double-sided tape that sticks to the beam on one side of the contact line and sticks to the bar at the other side of the line, see an impression in Fig. 12. The tape is loaded in tension throughout the whole motion, therefore a fiber-reinforced tape is very suitable.

C. Picture sequence

As an additional verification of the physical model, a weight has been applied at the intended point on the beam. This makes sense since this is the actual purpose of the design. A weight of $5.46kg$ is distributed at both sides of the

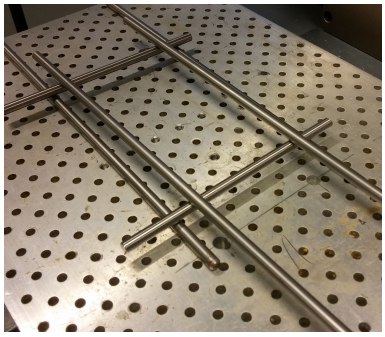

Fig. 10: Rollers setup used as planar bearing underneath the beam support structure.

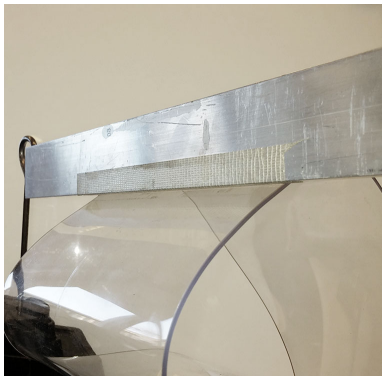

Fig. 11: Knife-edge bearing for the application of a vertical motion along a line of the surface. Double-sided tape holds the corner of the aluminum bar on its place.

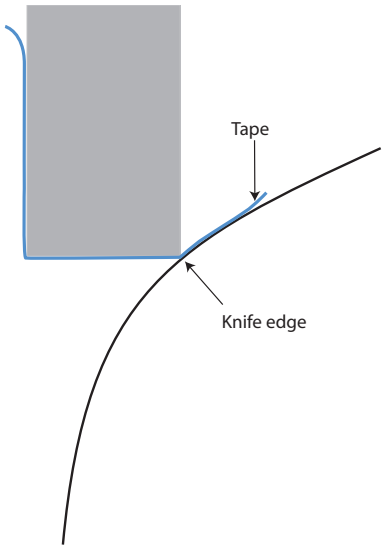

Fig. 12: Schematic of the tape holding the knife-edge bearing on its place on the surface of the beam.

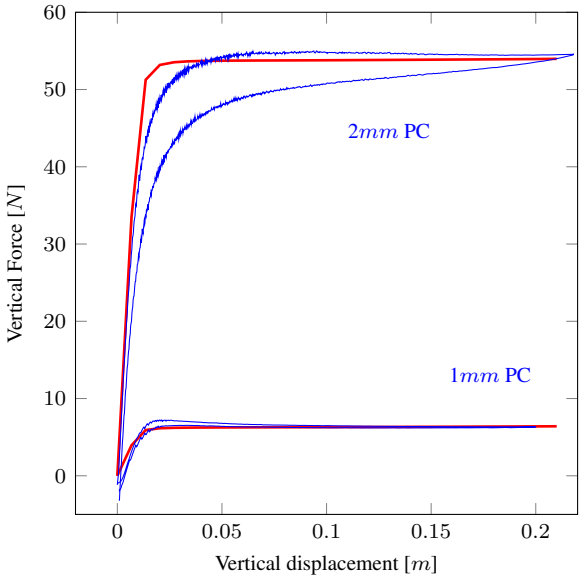

Fig. 13: Comparison of vertical force from the measurements and the model for both 1 mm and 2 mm thickness.

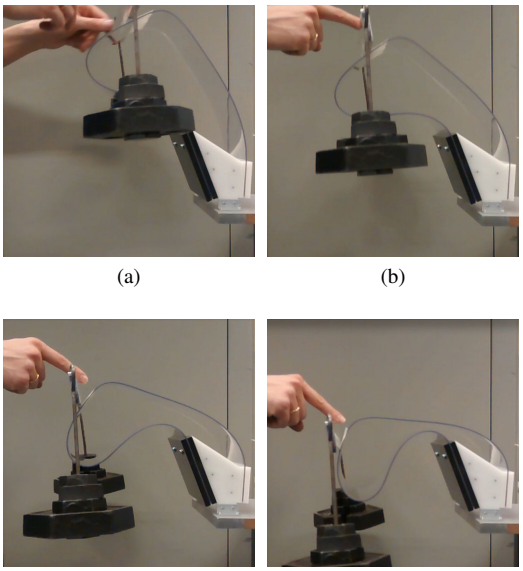

Fig. 14: Sequence of states of the system in downward movement. The spring approximately balances the attached weight over the range of motion.

beam and hang to the aluminum bar. By moving the bar down a bit and then release it, it can be verified whether the system stays motionless, i.e. in equilibrium, or whether it moves. A sequence of pictures is made that show the system in various configurations, see Fig. 14

V. Measurements results

The results of the measurements with the test bench are shown if Fig. 13, where the highest blue line is the force measured with the 2 mm plate in a forward and backward motion cycle. The lower blue line is the force measured on the 1 mm plate. In red the theoretical forces from the model are plotted for comparison.

Figure 14 shows a sequence of positions where the system stood still, indicating a stable or neutrally stable equilibrium situation. In downward direction the system stood still over most of its motion range and the movement required very little force, while in upward direction the system had the tendency to fall back and it clearly required a larger force to pull it up.

VI. Discussion

A. *Modelling/optimization*

The optimization works well as design aid for some special types of compliant mechanisms. The designed load-path, goal of the optimization, is very well accomplished by this approach. It is not trivial that by virtue of the shape of the beam only, such a near-perfect constant force can be generated by this elastic system.

Interesting to point out is the self searching behavior of the weight in horizontal direction. In fact the point of application of the payload does not need to be constrained over a particular path in order to achieve the desired behavior. The point is being moved vertically by imposing the displacement but will at every vertical step find the horizontal position of minimal energy for the system.

Even though the goal function of the optimization is known to be non-convex, thus not guarantying convergence to a global optimum, by use of a multi-start method enough satisfying local minima have been found. It must be noted that for this practical implementation, the guarantee of finding the global minimum is of no relevance, as long as the value of the local minimum is small enough in a practical sense. Since the goal function, by its definition, is lower-bounded at zero, finding the absolute zero is not better than finding a sufficiently small objective value. The threshold of good enough is of course a subjective matter and up to the user's insight and design requirements. Also it is wise to consider that the effect of a slightly higher goal function will in practice be overshadowed by imperfection of the physical system.

On the other hand it must be considered that, due to the high level of non-convexity, i.e. the presence of many local optima, it always remains unclear which minima were *not* found by the optimization. Did it miss some interesting, better, more efficient solutions? One where with less material a higher payload is balanced? Or one where the stresses in the material are distributed more evenly? These

questions are subjects of investigation which may lead to improved designs and procedures in future.

One aspect of the modeling that is known to produce an error is the offset from the control point on which the displacement is applied, with respect to the beam surface. However, in the resulting geometry and with applied refinement this offset is in the order of a tenth of a millimeter. This is considered insignificant for intended application, and especially compared to more significant manufacturing errors.

A choice made in the modeling steps is to remove the first few load-steps, in this case the first 5 out of 31. This is a deliberate choice of the designer that may influence the result to a large extend. The authors have chosen for a minimal amount, such that the ramp-up would be as steep as possible. Choosing a larger amount presumably simply results in good balancing properties but with a slower ramp-up and relatively a smaller range of motion. A smaller amount of steps has the risk that the first few steps that are not removed will influence the goal function too much in a negative sense, thus bringing the algorithm further away from potentially good results.

B. Prototype

In the current physical model which, as a preliminary construction has been made out of polycarbonate, it must be taken into consideration that this thermoplastic has a strongly nonlinear stress-strain characteristic. In the model however, a linear constitutive law has been adopted. Therefore an error in the measurements is to be expected that derives from this simplification. It can be observed that the 1 mm prototype seems to have a better match with the model, while the 2 mm prototype has a more rounded transition between the ramped part of the force and the constant part. This difference with the model, where the transition is clearly sharper, is considered to be related with nonlinearity of the material: The 2 mm version achieves higher strains and thus reaches further into the nonlinear stress-strain curve, while the 1 mm stays in the region where the stress-strain curve is considered linear.

Also the amount of hysteresis is considerably larger in the 2 mm prototype. It is known that internal losses within the material increase with increasing strain.

Furthermore, inaccuracies deriving from this particular production method must be taken into account. When the material sheet is cooling down, it shrinks due too thermal effects. This results in a curvature other than the designed curvature in the plane. Such curvature can have significant influence on the stiffness properties. As we know, a strip curved along its longitudinal direction, e.g. a tape measure, has totally different stiffness behavior than a flat strip.

Other issues source of inaccuracies will derive from the clamping of the beam onto its base. As the parts that clamp the beam are made out of laser-cut PMMA, they have a relatively low stiffness and exhibit a little amount of play.

C. Measurement

The measurement setup is simple and effective. It contains, except for the test bench, no particularly complex or expensive components. The support on rollers provides very low friction and high vertical stiffness of the support. Also the taped rectangular bar making the line-contact with the polycarbonate plate performs properly.

It can be noted from the measured data that there is a significantly higher noise in the beginning of the constant-force range. Even though the vertical force, and thus the load on the rollers, is nearly constant, the horizontal velocity of the base is significantly higher there and goes back to zero at the end of the range. As visible in Fig. 3 the point of applicatoin of the displacements almost describes an arc: horizontal at the start and vertical at the end. Also there is a sudden acceleration sideways at the very beginning of the motion due to the buckling behavior of the structure. Both the oscillations of the structure and the imperfections in the rollers result in higher noise under the described conditions of high acceleration and velocity.

The manual measurement where a weight is applied on the beam confirms the results from the testbench. In downward direction a large range of motion with constant force is found, while in upward direction, due the hysteresis, the system is always underbalanced.

VII. Conclusions

The paper presents a new monolithic, single branch, prismatic and compliant beam that balances a large weight over a large stroke with virtually perfect accuracy in the model. Moreover the system is self-searching in horizontal direction, i.e the point of application of the weight does not have to be constrained over a certain path or line.

The previously presented design method comprising a shape optimization procedure has been validated successfully by virtue of a non-trivial example. A rather complex shape was found that is able to exhibit a predefined complex behavior, i.e. large stroke constant force. Such a design challenge is not easily achieved with existing methods.

A physical model has been constructed for the validation of the results. A polycarbonate sheet has been thermoformed and draped onto a mould.

The experimental validation of the physical model has good resemblance with the prediction. The observed errors

have a predictable cause. Especially the non-linearity of the material, its internal hysteresis and the shape imperfection of the beam and the rollers are the main sources of errors.

Acknowledgment

The authors would like to acknowledge STW (HTSM-2012 12814: ShellMech) for the financial support of this project.

References

[1] Howell, L. L., 2001. *Compliant Mechanisms*. John Wiley and Sons Inc., New York,US.

[2] L. L. Howell and A. Midha, 1994. "A Method for the Design of Compliant Mechanisms With Small-Length Flexural Pivots". *Journal of Mechanical Design,* ***116***(1), pp. 280–290.

[3] Nianfeng, W., Xiaohe, L., and Xianmin, Z., 2014. "Pseudo-rigid-body model for corrugated cantilever beam used in compliant mechanisms". *Chinese Journal of Mechanical Engineering,* ***27***(1), pp. 122–129.

[4] Bandopadhya, D., Bhattacharya, B., and Dutta, A., 2009. "Pseudo-rigid body modeling of IPMC for a partially compliant four-bar mechanism for work volume generation". *Journal of Intelligent Material Systems and Structures,* ***20***(1), pp. 51–61.

[5] Herder, J. L., and van den Berg, F. P. A., 2000. "Statically balanced compliant mechanisms (SBCM's), an example and prospects". In Proceedings ASME DETC 26th Biennial Mechanisms and Robotics Conference.

[6] Vehar-Jutte, C., 2008. "Generalized Synthesis Methodology of Nonlinear Springs for Predescribed Load-Displacement Functions". PhD Thesis, The University of Michigan, Michigan, USA.

[7] Leishman, L. C., and Colton, M. B., 2011. "A pseudo-rigid-body model approach for the design of compliant mechanism springs for prescribed force-deflections". In Proceedings of ASME IDETC/CIE 2011, pp. 93–102.

[8] Merriam, E. G., Magleby, S., Colton, M., and Howell, L. L., 2013. "The design of a fully compliant statically balanced mechanism". In Proceedings of ASME IDETC/CIE 2013.

[9] Sönmez, Ü., and Tutum, C. C., 2008. "A compliant bistable mechanism design incorporating elastica buckling beam theory and pseudo-rigid-body model". *J. Mech. Des.,* ***130***(4), p. 042304.

[10] Radaelli, G., and Herder, J. L., 2014. "Isogeometric shape optimization for compliant mechanisms with prescribed load paths". In Proceedings ASME IDETC/CIE 2014.

[11] Radaelli, G., and Herder, J. L., 2014. "Shape sensitivity in isogeometric analysis of beams with prescribed load-path and large deformations". *Submitted to Int. J. Numer. Meth. Engng*.

[12] Hughes, T., Cottrell, J., and Bazilevs, Y., 2005. "Isogeometric analysis: Cad, finite elements, nurbs, exact geometry and mesh refinement". *Computer Methods in Applied Mechanics and Engineering,* ***194***(3941), pp. 4135 – 4195.

[13] Nagy, A. P., 2011. "Isogeometric Design Opitmization". PhD Thesis, Delft University of Technology, Delft, The Netherlands, December.